

Stable giant vortex annuli in microwave-coupled atomic condensates

Jieli Qin and Guangjiong Dong

*State Key Laboratory of Precision Spectroscopy, Department of Physics, East China Normal University, Shanghai 200062, China
and Collaborative Innovation Center of Extreme Optics, Shanxi University, Taiyuan, Shanxi 030006, China*

Boris A. Malomed

*Department of Physical Electronics, School of Electrical Engineering, Faculty of Engineering, Tel Aviv University, Ramat Aviv 69978, Israel
and Laboratory of Nonlinear-Optical Informatics, ITMO University, St. Petersburg 197101, Russia*

(Received 3 March 2016; revised manuscript received 17 October 2016; published 14 November 2016)

Stable self-trapped vortex annuli (VA) with large values of topological charge S (giant VA) not only are a subject of fundamental interest, but are also sought for various applications, such as quantum information processing and storage. However, in conventional atomic Bose-Einstein condensates (BECs) VA with $S > 1$ are unstable. Here we demonstrate that robust self-trapped fundamental solitons (with $S = 0$) and bright VA (with the stability checked up to $S = 5$) can be created in the free space by means of the local-field effect (the feedback of the BEC on the propagation of electromagnetic waves) in a condensate of two-level atoms coupled by a microwave (MW) field, as well as in a gas of MW-coupled fermions with spin $1/2$. The fundamental solitons and VA remain stable in the presence of an arbitrarily strong repulsive contact interaction (in that case, the solitons are constructed analytically by means of the Thomas-Fermi approximation). Under the action of the attractive contact interaction with strength β , which, by itself, would lead to collapse, the fundamental solitons and VA exist and are stable, respectively, at $\beta < \beta_{\max}(S)$ and $\beta < \beta_{\text{st}}(S)$, with $\beta_{\text{st}}(S = 0) = \beta_{\max}(S = 0)$ and $\beta_{\text{st}}(S \geq 1) < \beta_{\max}(S \geq 1)$. Accurate analytical approximations are found for both β_{st} and β_{\max} , with $\beta_{\text{st}}(S)$ growing linearly with S . Thus, higher-order VA are more robust than their lower-order counterparts, in contrast to what is known in other systems that may support stable self-trapped vortices. Conditions for the experimental realizations of the VA are discussed.

DOI: [10.1103/PhysRevA.94.053611](https://doi.org/10.1103/PhysRevA.94.053611)**I. INTRODUCTION**

Light and microwaves (MWs) are important tools for controlling the dynamics of atomic Bose-Einstein condensates (BECs). In addition to creating traps and optical lattices [1], various optical patterns, including vortices, have potential application in the realm of quantum data processing, as the light patterns can be stored in the form of intrinsic atomic states in BECs and released back in the optical form [2]. Furthermore, light can generate entangled vortices in separated condensates [3].

The BEC feedback on the light propagation, i.e., the local field effect (LFE), may lead to the creation of hybrid light-matter states [4–9]. The electric LFE explains asymmetric matter-wave diffraction [4,10] and predicts polaritonic solitons in soft optical lattices [5]. Further, the magnetic LFE couples MWs to a pseudospinor (two-component) BEC of two-level atoms, thus opening the way to the creation of hybrid microwave-matter-wave solitons [6]. On the other hand, in current experiments with the pseudospinor BECs, atoms are first transferred to an intermediate level using a MW field and then further driven to a target level using a radiofrequency field, which would not allow one to observe manifestations of the magnetic LFE. This should become possible if the experiments can be performed with the MW field directly transferring the atoms between the two relevant states.

The LFE plays an increasingly important role in BECs with an increase of the number of atoms, which can exceed 10^8 , as predicted theoretically [11] and demonstrated experimentally [12], allowing the LFE-induced long-range interactions

between atoms [5,6] to produce new manifestations of nonlocal physics. Actually, the long-range interaction may cover the whole gas, in contrast with fast-decaying nonlocal interactions in optics [13] and in dipolar BECs [14–19]. Unlike the species-dependent dipolar forces [14–17], the LFE-induced interaction can be realized in any ultracold atomic or molecular gas [6].

The LFE was not previously explored in two- and three-dimensional (3D) settings, where it may give rise to new phenomenology in comparison with the recently investigated 1D case [4–6], as the LFE-induced interaction is determined by the underlying Green's function, which has different forms in effectively 1D, 2D, and 3D geometries (note that the above-mentioned “massive” BEC, with a large number of atoms $\gtrsim 10^8$, can be readily morphed into a low-dimensional shape [12]). In particular, we demonstrate here that solitary vortices, alias vortex annuli (VA), readily self-trap in the 2D setting. Vortices in BECs are essential for simulating various effects originating in condensed matter [20] and as building blocks of quantum turbulence [21]. They also help to emulate gravitational physics [22] and find applications such as phase qubits [23] and matter-wave Sagnac interferometers for testing the rotational-equivalence principle [24–26]. As mentioned above, atomic-matter vortices can store and release information delivered by optical vortex beams [2].

The stabilization of VA with large values of the topological charge (vorticity) S , which is required for deterministic creation of vortices [27] and for applications (in particular, the storage of higher-order optical vortices in the form of their atomic counterparts), is a challenging issue [28].

Under repulsive interactions, vortices supported by a nonzero background are stable solely for $S = 1$, while vortices with $S \geq 2$ split into ones with $S = 1$ [28]. For the above-mentioned applications, most relevant are bright VA in BECs with attractive nonlinearity. Unlike nonlinear optics, where VA can be stabilized by non-Kerr nonlinearities [29], in BECs with attractive interactions the only setting that gives rise to stable 2D [30] and 3D [31] semivortices (with $S_\uparrow = 1$ and $S_\downarrow = 0$ in their two components) in the free space is provided by the spin-orbit coupling. However, all higher-order states, with $S_\uparrow = 1 + s$ and $S_\downarrow = s \geq 1$, are unstable. The family of single-component modes with $S = 1$ may be partly stabilized by a trapping potential, but all the higher-order VA with $S \geq 2$ remain unstable in this case too [32]. Partly stable VA with $S \geq 2$ were predicted only in exotic settings, with the local strength of the repulsive nonlinearity in the space of dimension D growing with distance r from the center faster than r^D [33], or making use of a combination of a trapping potential and a spatially localized attractive interaction [34].

In this work we introduce a 2D hybrid system consisting of a pseudospinor BEC whose two components are coupled by a MW field through a magnetic dipole transition. The system gives rise to stable giant VA, i.e., ones with arbitrarily high values of S (the stability checked up to $S = 5$). This is also possible in the presence of additional contact repulsive interactions. On the other hand, under the action of an attractive contact interaction, with strength β , which drives the critical collapse in the 2D geometry [35], the VA exist and are stable, respectively, for $\beta < \beta_{\max}$ and $\beta < \beta_{\text{st}} \leq \beta_{\max}$. We demonstrate, by means of analytical and numerical considerations, that β_{st} linearly grows with S , thus making higher-order vortices more robust than lower-order ones, opposite to what is known in a few other models capable of supporting stable higher-order VA [33,34]. It is relevant to mention that the concept of giant vortices is known in the usual BEC settings with the contact repulsion [36], where they are not self-trapped objects, i.e., they are not VA.

The rest of the paper is organized as follows. The model is introduced in Sec. II, numerical and analytical results are collected in Sec. III, and a summary is given in Sec. IV.

II. MODEL

As schematically shown in Fig. 1, we consider a nearly 2D (pancake-shaped) binary BEC composed of two different hyperfine states of the same atomic species, which is described by the two-component (pseudospinor) wave function $|\Psi\rangle = (\Psi_\downarrow, \Psi_\uparrow)^T$, with each component emulating spin-up and spin-down states. The corresponding Hamiltonian is $\mathcal{H} = \hat{\mathbf{p}}^2/2m_{\text{at}} - (\hbar\delta/2)\sigma_3 - \mathbf{m} \cdot \mathbf{B}$ [6], where m_{at} , $\hat{\mathbf{p}}$, and \mathbf{m} are the atomic mass, 2D momentum, and magnetic moment, respectively, $\hbar\delta$ is an energy difference between atomic states $|\uparrow\rangle$ and $|\downarrow\rangle$, σ_3 is the Pauli matrix, and $\mathbf{B} = \mu_0(\mathbf{H} + \mathbf{M})$ is the magnetic induction, with magnetic field \mathbf{H} and magnetization $\mathbf{M} = \langle\Psi|\mathbf{m}|\Psi\rangle$. In the rotating-wave approximation, the atomic wave function $|\psi\rangle \equiv |\phi\rangle e^{\pm i\omega t/2} \equiv (\phi_\downarrow, \phi_\uparrow)^T$ is governed by coupled Gross-Pitaevskii equations (GPEs) (with an asterisk standing for the complex

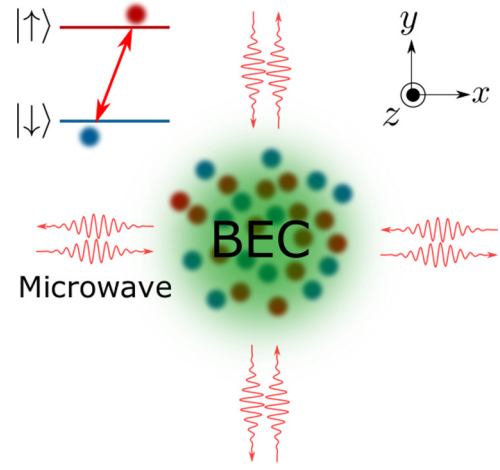


FIG. 1. Two hyperfine atomic states coupled by the MW field in a pancake-shaped BEC. The MW field is polarized in the direction perpendicular to the pancake's plane.

conjugate)

$$\begin{aligned} i\hbar\partial\phi_\downarrow/\partial t &= (\hat{\mathbf{p}}^2/2m_{\text{at}} + \hbar\Delta/2 - \mu_0\mathbf{m}_{\uparrow\downarrow} \cdot \mathbf{m}_{\downarrow\uparrow}|\phi_\downarrow|^2)\phi_\downarrow \\ &\quad - \mu_0\mathbf{m}_{\downarrow\uparrow} \cdot \mathbf{H}\phi_\uparrow, \\ i\hbar\partial\phi_\uparrow/\partial t &= (\hat{\mathbf{p}}^2/2m_{\text{at}} - \hbar\Delta/2 - \mu_0\mathbf{m}_{\uparrow\downarrow} \cdot \mathbf{m}_{\downarrow\uparrow}|\phi_\uparrow|^2)\phi_\uparrow \\ &\quad - \mu_0\mathbf{m}_{\uparrow\downarrow} \cdot \mathbf{H}\phi_\downarrow, \end{aligned} \quad (1)$$

with detuning $\Delta = \omega - \delta$ of the MW from the atomic transition and matrix elements of the magnetic moment $\mathbf{m}_{\uparrow\downarrow}$ and $\mathbf{m}_{\downarrow\uparrow}$ ($\mathbf{m}_{\uparrow\uparrow} = \mathbf{m}_{\downarrow\downarrow} = 0$ due to the symmetry).

The magnetic field and magnetization, which are polarized perpendicular to the pancake's plane, are each represented by a single component H and M , which obey the Helmholtz equation

$$\nabla^2 H + k^2 H = -k^2 M, \quad (2)$$

where k is the MW wave number. As the wavelength of the MW field $\lambda = 2\pi/k$ is always much greater than an experimentally relevant size of the BEC, the second term in Eq. (2) may be omitted in comparison with the first term (see also Ref. [6]), reducing Eq. (2) to the Poisson equation for the scalar field

$$\nabla^2 H = -k^2 M. \quad (3)$$

Because the medium's magnetization, which is the source of the magnetic field, is concentrated in the pancake, the Poisson equation may be treated as one in the 2D plane. Then using the Green's function of the 2D Poisson equation, the magnetic field is given by

$$H = H_0 - Nk^2|\mathbf{m}_{\downarrow\uparrow}|/2\pi l_\perp \int \ln(|\mathbf{r} - \mathbf{r}'|)\phi_\downarrow^*(\mathbf{r}')\phi_\uparrow(\mathbf{r}')d\mathbf{r}', \quad (4)$$

where H_0 is a background magnetic field of the MW, N is the number of atoms, and \mathbf{r} is the set of 2D coordinates normalized by the transverse confinement size l_\perp . The GPEs for the wave function, subject to normalization $\int(|\phi_\uparrow|^2 + |\phi_\downarrow|^2)d\mathbf{r} = 1$, take the

form

$$i \frac{\partial \phi_{\downarrow}}{\partial \tau} = \left(-\frac{1}{2} \nabla^2 + \eta + H_0 - \beta |\phi_{\uparrow}|^2 \right) \phi_{\downarrow} + \frac{\gamma \phi_{\uparrow}}{2\pi} \int \ln(|\mathbf{r} - \mathbf{r}'|) \phi_{\downarrow}(\mathbf{r}') \phi_{\uparrow}^*(\mathbf{r}') d\mathbf{r}', \quad (5)$$

$$i \frac{\partial \phi_{\uparrow}}{\partial \tau} = \left(-\frac{1}{2} \nabla^2 - \eta + H_0 - \beta |\phi_{\downarrow}|^2 \right) \phi_{\uparrow} + \frac{\gamma \phi_{\downarrow}}{2\pi} \int \ln(|\mathbf{r} - \mathbf{r}'|) \phi_{\downarrow}^*(\mathbf{r}') \phi_{\uparrow}(\mathbf{r}') d\mathbf{r}', \quad (6)$$

where rescaling is defined by $\phi_{\uparrow,\downarrow} = \sqrt{N}/l_{\perp} \psi_{\uparrow,\downarrow}$, $\tau = t/t_0$ with $t_0 = \hbar/E_c$ and $E_c = \hbar^2/m_{\text{at}} l_{\perp}^2$, $\eta \equiv t_0 \Delta/2$, and scaled strengths of the LFE and contact interactions (if any) are

$$\gamma = m_{\text{at}} l_{\perp} k^2 N \mu_0 |\mathbf{m}_{\downarrow\uparrow}|^2 / \hbar^2, \quad \beta \equiv N \mu_0 \mathbf{m}_{\uparrow\downarrow} \cdot \mathbf{m}_{\downarrow\uparrow} / \hbar l_{\perp}^3 E_c. \quad (7)$$

To describe experimental conditions, three-dimensional settings should also include the trapping potential $(\Omega^2/2)r^2\phi_{\uparrow,\downarrow}$. It has been checked that, after the creation of the trapped modes, the potential may be switched off, leading to a smooth transformation of the modes into their self-trapped counterparts, obtained directly in the free space ($\Omega = 0$). The vorticity may be imparted to the trapped condensate by a vortical optical beam [2].

If collisions between atoms belonging to the two components are considered (with the corresponding strength of the contact interaction tunable by dint of the Feshbach resonance [37]), the additional cross-cubic terms can be absorbed into the rescaled coefficient β . Collisions may also give rise to self-interaction terms $-\tilde{\beta}|\phi_{\downarrow}|^2$ and $-\tilde{\beta}|\phi_{\uparrow}|^2$ in the large parentheses of Eqs. (5) and (6), respectively. On the other hand, the same equations with $\tilde{\beta} = 0$ apply as well to a different physical setting, viz., a degenerate Fermi gas with spin $\frac{1}{2}$, in which ϕ_{\downarrow} and ϕ_{\uparrow} represent two spin components, coupled by the MW magnetic field [6,38].

The following analysis is chiefly dealing with the zero-detuning (symmetric) system, $\eta = 0$. In this case, Eqs. (5) and (6) coalesce into a single equation for $\phi_{\downarrow} = \phi_{\uparrow} \equiv \phi \exp(-iH_0\tau)$, subject to normalization $\int |\phi(\mathbf{r})|^2 d\mathbf{r} = \frac{1}{2}$,

$$i \frac{\partial \phi}{\partial \tau} = \left[-\frac{1}{2} \nabla^2 - \beta |\phi|^2 + \frac{\gamma}{2\pi} \int \ln(|\mathbf{r} - \mathbf{r}'|) |\phi(\mathbf{r}')|^2 d\mathbf{r}' \right] \phi, \quad (8)$$

and the above-mentioned self-interaction coefficient $\tilde{\beta}$ may be absorbed into β . This equation and the normalization condition are invariant with respect to the self-similarity transformation, $\phi(\mathbf{r}, \tau) = \sqrt{\gamma_0} \tilde{\phi}(\tilde{\mathbf{r}}, \tilde{\tau}) \exp\{-i[\gamma(\ln \gamma_0)/8\pi]\tau\}$, $\tau = \gamma_0^{-1} \tilde{\tau}$, $\mathbf{r} = \gamma_0^{-1/2} \tilde{\mathbf{r}}$, $\gamma = \gamma_0 \tilde{\gamma}$, and $\beta \equiv \tilde{\beta}$, which allows one to replace γ by γ/γ_0 with an arbitrary factor γ_0 . We use this option to set $\gamma = \pi$ in the numerical analysis of the symmetric configuration. In physical units, for alkali-metal atoms transversely confined with $l_{\perp} = 1 \mu\text{m}$ and irradiated by a MW with a wavelength of 1 mm, the above definition yields $\gamma \sim 10^{-7} N$. Thus, $\gamma \sim 10$ for the experimentally available massive BEC with $N \sim 10^8$ [11,12], while a typical vortex annulus radius can be estimated as $\sim 10 \mu\text{m}$ (see Figs. 2

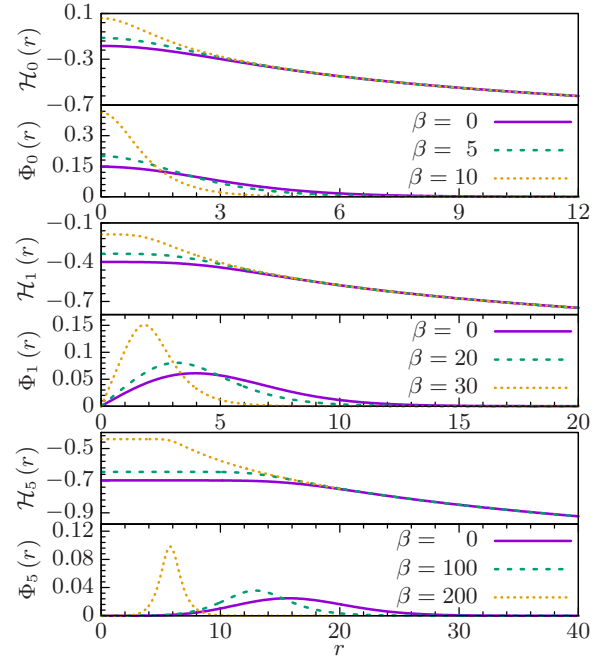


FIG. 2. Radial profiles of the magnetic field and wave functions in fundamental solitons (top) and vortices with $S = 1$ (middle) and $S = 5$ (bottom) at indicated values of β .

and 5 below) and a characteristic range of the magnetic-field amplitudes may reach a few gauss.

III. RESULTS

Stationary solutions to Eq. (8) with chemical potential μ and vorticity S are looked for, in polar coordinates (r, θ) , as

$$\phi = e^{-i\mu\tau - iS\theta} \Phi_S(r), \quad (9)$$

where $\Phi_S(r)$ is a real radial wave function. Typical examples of solutions for $\Phi_S(r)$, produced by the imaginary-time evolution method [39], are plotted in Fig. 2 for different values of S and $\beta \geq 0$. Numerical results demonstrate that fundamental solitons (which correspond to $S = 0$) and VA are destroyed by the collapse at $\beta > \beta_{\text{max}}(S)$ (see Table I). This critical value can be found by considering the energy corresponding to Eqs. (5)

TABLE I. Numerically obtained β_{max} and analytically predicted $\beta_{\text{max}}^{(\text{an})}$ values of the contact-interaction strength β , up to which the fundamental solitons and vortex annuli exist, and β_{st} , the numerically identified stability boundary of the vortex annuli.

S	β_{max}	$\beta_{\text{max}}^{(\text{an})}$	β_{st}
0	11.8		$\equiv \beta_{\text{max}}$
1	48.3	43.5	11
2	89.7	87.0	28
3	132.5	130.6	41
4	175.5	174.1	57
5	218.5	217.7	70

and (6) with $\phi_{\uparrow} = \phi_{\downarrow}$,

$$E = 2\pi \int_0^{\infty} r dr [(\Phi'_S)^2 + r^{-2} S^2 \Phi_S^2 - \beta \Phi_S^4] + \frac{\gamma}{2\pi} \iint d\mathbf{r}_1 d\mathbf{r}_2 \ln(|\mathbf{r}_1 - \mathbf{r}_2|) \Phi_S^2(\mathbf{r}_1) \Phi_S^2(\mathbf{r}_2). \quad (10)$$

The numerical findings displayed in Figs. 2 and 5 suggest that, for $S \geq 2$ and β large enough, the vortex takes the shape of a narrow annulus, which may be approximated by the usual quasi-1D soliton shape in the radial direction, with regard to the adopted normalization (cf. Ref. [40]):

$$\Phi_S(r) = \sqrt{\beta/8\pi R} \operatorname{sech}[\beta(r - R)/8\pi R], \quad (11)$$

where R is the radius of the vortex annulus. The substitution of this approximation in Eq. (10) yields

$$E(R) = \left[S^2 - \frac{\beta^2}{3(8\pi)^2} \right] \frac{1}{2R^2} + \frac{\gamma}{8\pi} \ln R. \quad (12)$$

Next, the annulus's radius R is to be selected as a point corresponding to the energy minimum: $dE/dR = 0$, i.e., $R_{\min}^2 = (8\pi/\gamma)[S^2 - \frac{1}{3}(\beta/8\pi)^2]$ (a comparison with numerical results demonstrates that R_{\min} provides a reasonable approximation for the radius of narrow VA). Then β_{\max} is predicted as the value at which R_{\min}^2 vanishes, i.e., the annulus collapses to the center

$$\beta_{\max}^{(\text{an})} = 8\sqrt{3}\pi S. \quad (13)$$

As can be seen in Table I, this analytical prediction is virtually identical to its numerically found counterparts for $S \geq 2$.

Further, it is found that β_{\max} is the same as in the ‘‘simplified’’ 2D GPE that contains solely the local-attraction term

$$i\partial\phi/\partial\tau = -\left[\frac{1}{2}\nabla^2 + \beta|\phi|^2\right]\phi \quad (14)$$

for which the existence limit was found in Ref. [41], for $S = 0$, and in Ref. [42] for $1 \leq S \leq 5$, i.e., β_{\max} does not depend of the LFE strength γ . To explain this fact, we note that, at the limit stage of the collapse, when the shrinking 2D annulus becomes extremely narrow, the equation for the wave function becomes asymptotically tantamount to Eq. (14), therefore the condition for the onset of the collapse is identical in both equations. However, the solitons of Eq. (14) exist solely at $\beta = \beta_{\max}$, which is completely unstable, while the LFE-induced long-range interaction in Eqs. (5) and (6) creates stable solitons and vortices for all S , as shown below. It is worth stressing too that the analytical result given by Eq. (13) provides an explanation for the numerical findings that were first reported in Ref. [42] and later considered in many works, but never reproduced in an analytical form.

The stability of the self-trapped modes has been systematically tested by real-time simulations of Eqs. (5) and (6) with random perturbations added to the stationary solutions (independent perturbations were taken for ϕ_{\uparrow} and ϕ_{\downarrow} to verify the stability against breaking the symmetry between them). The fundamental solitons are stable in their entire existence region $\beta < \beta_{\max} \approx 11.8$. At β very close to β_{\max} , the perturbations lead to persistent oscillations, as shown in Fig. 3(a) for $\beta = 11.6$, due to excitation of a soliton's internal mode [43–46]. It can be seen in Fig. 3(b) that the oscillation

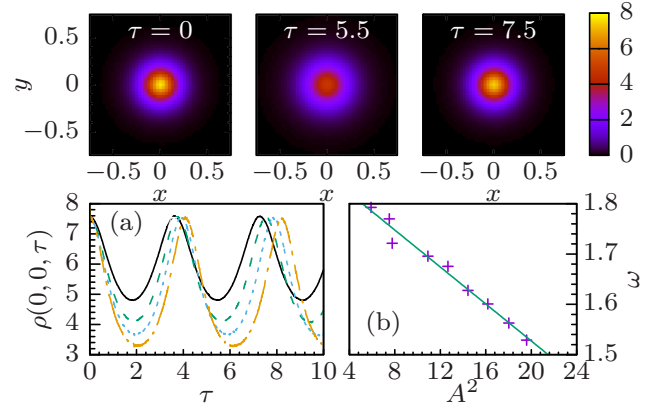


FIG. 3. (a) Oscillations of the peak density $\rho(0,0) \equiv |\phi_{\downarrow}(x = y = 0)|^2 + |\phi_{\uparrow}(x = y = 0)|^2$ of the perturbed fundamental soliton at $\beta = 11.6$ (for different perturbation amplitudes). (b) Oscillation frequency vs the squared oscillation amplitude A^2 . The top row displays profiles of the oscillating soliton.

frequency is a nearly linear function of the squared amplitude of the oscillations, which is a typical feature of a nonlinear oscillatory mode.

Systematic simulations of the evolution of the families of VA reveal an internal stability boundary $\beta_{\text{st}}(S) < \beta_{\max}(S)$ (see Table I), the vortices being stable at $\beta < \beta_{\text{st}}(S)$. In the interval of $\beta_{\text{st}}(S) < \beta < \beta_{\max}(0)$, they are broken by azimuthal perturbations into rotating necklace-shaped sets of fragments, which resembles the initial stage of the instability development of localized vortices in usual models [29,32,47,48]; however, unlike those models, the necklace does not expand, remaining confined under the action of the effective nonlocal interaction. Typical examples of the stable and unstable evolution of fundamental solitons and VA are displayed, respectively, in Figs. 4 and 5.

To address the stability of the VA against azimuthal perturbations in an analytical form, we approximate the wave function of a perturbed vortex annulus by $A(\theta)\Phi_S(r)$ and derive an evolution equation for the modulation amplitude

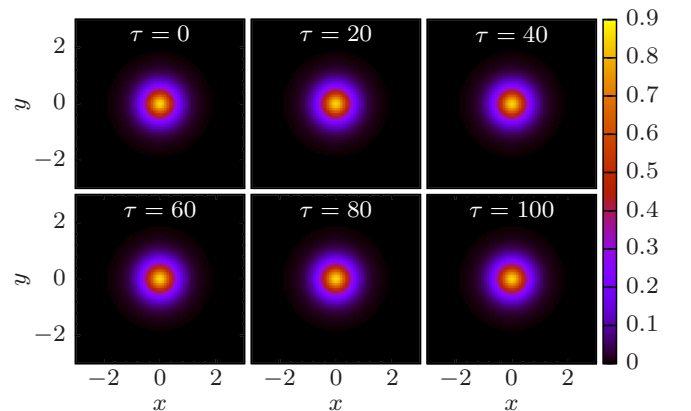


FIG. 4. Stable perturbed evolution of the fundamental soliton, with $S = 0$ and $\beta = 11$. Note that this value of β is close to the existence boundary $\beta_{\max}(S = 0) = 11.8$ (see Table I).

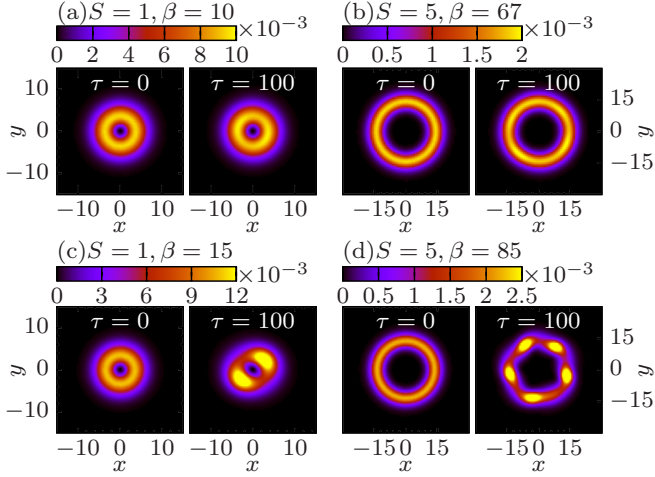


FIG. 5. Examples of the (a) and (b) stable and (c) and (d) unstable perturbed evolution of the VA with indicated values of S and β . The necklace-shaped set, observed in the latter case, remains confined (keeping the same overall radius) in the course of subsequent evolution.

A by averaging Eqs. (5) and (6) in the radial direction:

$$i \frac{\partial A}{\partial \tau} = -\frac{1}{2R^2} \frac{\partial^2 A}{\partial \theta^2} + \left[\frac{\gamma \ln R}{4\pi R} - \frac{2\beta^2}{3(8\pi R)^2} \right] |A|^2 A. \quad (15)$$

A straightforward analysis of the modulational stability of the solution with $A = 1$ against perturbations $\sim \exp(ip\theta)$ with integer winding numbers p [49] shows that the stability is maintained under the threshold condition $p^2 \geq \frac{8}{3}(\beta/8\pi)^2$ if the term $\sim \beta^2$ dominates in Eq. (15). Further, the numerical results demonstrate that, as in other models [29,50], the critical instability corresponds to $p^2 = S^2$ (for instance, the appearance of five fragments in the part of Fig. 5 corresponding to $S = 5$ and $\beta = 85$ demonstrates that, for $S = 5$, the dominant splitting mode has $p = 5$). Thus, it is expected that the VA remain stable at $\beta < \beta_{st}^{(an)}(S) = 2\sqrt{6}\pi S \approx 15.4S$. On the other hand, the numerically found stability limits collected in Table I obey an empirical formula $\beta_{st}^{(num)}(S) \approx 15S - 4$. Thus, the analytical approximation is quite accurate for $S \geq 2$. To put this result in a physical context, we note that, in terms of experimentally relevant parameters, the scaling adopted above implies $|\beta| \sim (|a_s|/L_\perp)N$, where $a_s < 0$ is the scattering length that accounts for the contact attraction. Thus, values of β (actually, of either sign) may be relevant up to $|\beta| \sim 1000$.

It follows from these results that the giant VA, with higher values of S , are much more robust than their counterparts with smaller S . This feature is opposite to what was previously found in those (few) models that are able to produce stable VA with $S > 1$ [29,33,34]. It is relevant to mention that, at $\beta < \beta_{st}(S = 0)$, the fundamental soliton is the system's ground state, while at $\beta > \beta_{st}(S = 0)$, the ground state does not exist, due to the possibility of the collapse. The vortices with $\beta_{st}(S) > \beta$ cannot represent the ground state, but they exist as metastable ones (cf. the spin-orbit-coupled system, considered in Ref. [31], where self-trapped three-dimensional modes of the semivortex type exist too as metastable states, although the

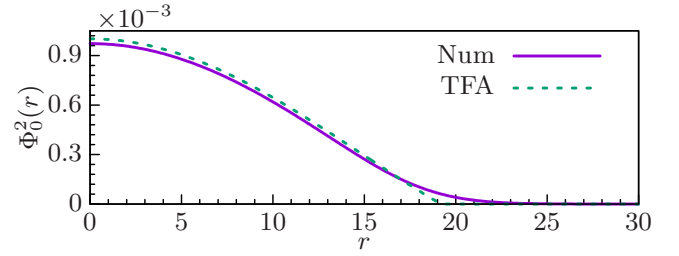


FIG. 6. Comparison of the Thomas-Fermi approximation, as given by Eq. (16), for the fundamental soliton (dashed line) and its numerically found counterpart (solid line), for $\beta = -200$.

system does not have a ground state, due to the presence of the supercritical collapse).

For the strong repulsive contact interaction (large $\beta < 0$), fundamental solitons (with $S = 0$) can be constructed by means of the Thomas-Fermi approximation (TFA), as shown by straightforward consideration of the stationary version of Eq. (8), with the substitution of the stationary wave form as per Eq. (9). In this case, it is more convenient, instead of using the Green's function, to explicitly combine the stationary equation with Poisson equation (3). The result is

$$(\Phi_0^2)_{TFA}(r) = \begin{cases} \phi_0^2 J_0(\xi r) & \text{for } r < r_1/\xi \\ (\Phi_0^2)_{TFA}(r) = 0 & \text{for } r > r_1/\xi, \end{cases} \quad (16)$$

where $\xi \equiv \sqrt{\gamma/|\beta|}$, $r_1 \approx 2.4$ is the first zero of the Bessel function $J_0(r)$, and ϕ_0 is a normalization constant. Figure 6 shows that the TFA agrees very well with the numerical solution.

Finally, it is relevant to proceed from the symmetric system [$\eta = 0$ and $\phi_\uparrow = \phi_\downarrow$ in Eqs. (5) and (6)] to a strongly asymmetric one, with large η . The relevant solution has $\mu = -\eta + \delta\mu$ with $|\delta\mu| \ll \eta$ and a small component $\Phi_\downarrow \approx (H_0/2\eta)\Phi_\uparrow$, while the large one satisfies the equation

$$\left(\Delta\mu + \frac{H_0^2}{2\eta} \right) \Phi_\uparrow = -\frac{1}{2} \nabla^2 \Phi_\uparrow - \frac{\beta H_0^2}{4\eta^2} \Phi_\uparrow^3 - \frac{\gamma H_0^2}{8\pi\eta^2} \Phi_\uparrow \times \int \ln(|\mathbf{r} - \mathbf{r}'|) \Phi_\uparrow^2(\mathbf{r}') d\mathbf{r}'. \quad (17)$$

Up to obvious rescaling, Eq. (17) is identical to the equation for the stationary wave function in the symmetric case, i.e., Eq. (8) with substitution of the wave function as per Eq. (9), with any value of S . Thus, the strongly asymmetric solutions can be obtained by means of the rescaling of their symmetric counterparts.

IV. CONCLUSION

In this work we have developed the analysis for the 2D fundamental solitons and vortex annuli produced by the local field effect in the BEC composed of two-level atoms or, alternatively, a gas of fermions, in which two components are coupled by the microwave field. The effective long-range interaction mediated by the field stabilizes the solitons and VA, even in the presence of the attractive contact interaction between the two components, which, by itself, leads to the critical collapse. The solitons exist too and are stable

in the presence of the arbitrarily strong contact repulsion. Nearly exact critical values of the local-attraction strength β_{\max} , up to which the solitons and vortices exist, have been found analytically. This result also provides an analytical explanation for the well-known existence limits of VA in the 2D nonlinear Schrödinger–Gross-Pitaevskii equation with the cubic self-focusing term, which were previously known solely in the numerical form. While the fundamental solitons are stable up to $\beta = \beta_{\max}$, the VA remain stable in a smaller interval $\beta \leq \beta_{\text{st}} < \beta_{\max}$, being vulnerable to the azimuthal instability at $\beta_{\text{st}} < \beta < \beta_{\max}$. The stability boundary β_{st} is found in an approximate analytical form too. Contrary to previously studied models [29,33,34], the (giant) VA with higher vorticities, such as $S = 5$, are more robust than their counterparts with small S . In addition, a very accurate Thomas-Fermi approximation was developed for the fundamental solitons, with $S = 0$. The results have been obtained for both symmetric and strongly asymmetric two-component systems.

The VA obtained here can be further used to construct vortex lattices [51]. Challenging possibilities are to consider

the interaction between the self-trapped modes and eventually to extend the model to the fully 3D setting. Another direction for the extension of the work is to explore the electric LFE in a molecular condensate.

ACKNOWLEDGMENTS

This work was supported, in part, by the National Science Foundation of China (Grants No. 11574085 and No. 91536218), the Research Fund for the Doctoral Program of Higher Education of China (Grant No. 20120076110010), the Program of Introducing Talents of Discipline to Universities (No. B12024), and by the joint program in physics between the National Science Foundation (US) and Binational Science Foundation (US-Israel), through Grant No. 2015616. B.A.M. appreciates hospitality of the State Key Laboratory of Precision Spectroscopy and the Department of Physics at the East China Normal University.

-
- [1] C. S. Adams, M. Sigel, and J. Mlynek, *Phys. Rep.* **240**, 143 (1994); G. Grynberg and C. Robilliard, *ibid.* **355**, 335 (2001); V. A. Brazhnyi and V. V. Konotop, *Mod. Phys. Lett. B* **18**, 627 (2004); O. Morsch and M. Oberthaler, *Rev. Mod. Phys.* **78**, 179 (2006); I. Bloch, J. Dalibard, and W. Zwerger, *ibid.* **80**, 885 (2008); S. Giorgini, L. P. Pitaevskii, and S. Stringari, *ibid.* **80**, 1215 (2008).
- [2] M. F. Andersen, C. Ryu, P. Cladé, V. Natarajan, A. Vaziri, K. Helmerson, and W. D. Phillips, *Phys. Rev. Lett.* **97**, 170406 (2006); R. Pugatch, M. Shuker, O. Firstenberg, A. Ron, and N. Davidson, *ibid.* **98**, 203601 (2007); M. Shuker, O. Firstenberg, R. Pugatch, A. Ron, and N. Davidson, *ibid.* **100**, 223601 (2008).
- [3] N. Lo Gullo, S. McEndoo, T. Busch, and M. Paternostro, *Phys. Rev. A* **81**, 053625 (2010).
- [4] J. Zhu, G. J. Dong, M. N. Shneider, and W. Zhang, *Phys. Rev. Lett.* **106**, 210403 (2011).
- [5] G. J. Dong, J. Zhu, W. Zhang, and B. A. Malomed, *Phys. Rev. Lett.* **110**, 250401 (2013).
- [6] J. L. Qin, G. J. Dong, and B. A. Malomed, *Phys. Rev. Lett.* **115**, 023901 (2015).
- [7] F. Cattani, A. Kim, M. Lisak, and D. Anderson, *Int. J. Mod. Phys. B* **27**, 1330003 (2013).
- [8] G. Labeyrie, E. Tesio, P. M. Gomes, G.-L. Oppo, W. J. Firth, G. R. M. Robb, A. S. Arnold, R. Kaiser, and T. Ackemann, *Nat. Photon.* **8**, 321 (2014).
- [9] J. T. Mendonça and R. Kaiser, *Phys. Rev. Lett.* **108**, 033001 (2012).
- [10] K. Li, L. Deng, E. W. Hagley, M. G. Payne, and M. S. Zhan, *Phys. Rev. Lett.* **101**, 250401 (2008).
- [11] D. Comparat, A. Fioretti, G. Stern, E. Dimova, B. Laburthe Tolra, and P. Pillet, *Phys. Rev. A* **73**, 043410 (2006).
- [12] K. M. van der Stam, E. D. van Ooijen, R. Meppelink, J. M. Vogels, and P. van der Straten, *Rev. Sci. Instrum.* **78**, 013102 (2007); H. Imai, T. Akatsuka, T. Ode, and A. Morinaga, *Phys. Rev. A* **85**, 013633 (2012).
- [13] R. Barboza, U. Bortolozzo, M. G. Clerc, S. Residori, and E. Vidal-Henriquez, *Adv. Opt. Photon.* **7**, 635 (2015).
- [14] A. Griesmaier, J. Werner, S. Hensler, J. Stuhler, and T. Pfau, *Phys. Rev. Lett.* **94**, 160401 (2005).
- [15] M. Lu, N. Q. Burdick, S. H. Youn, and B. L. Lev, *Phys. Rev. Lett.* **107**, 190401 (2011); M. Lu, N. Q. Burdick, and B. L. Lev, *ibid.* **108**, 215301 (2012).
- [16] K. Aikawa, A. Frisch, M. Mark, S. Baier, A. Rietzler, R. Grimm, and F. Ferlaino, *Phys. Rev. Lett.* **108**, 210401 (2012); K. Aikawa, A. Frisch, M. Mark, A. Baier, R. Grimm, and F. Ferlaino, *ibid.* **112**, 010404 (2014).
- [17] K.-K. Ni, S. Ospelkaus, M. H. G. de Miranda, A. Pe'er, B. Neyenhuis, J. J. Zirbel, S. Kotochigova, P. S. Julienne, D. S. Jin, and J. Ye, *Science* **322**, 231 (2008); J. Deiglmayr, A. Grochola, M. Repp, K. Mörtlbauer, C. Glück, J. Lange, O. Dulieu, R. Wester, and M. Weidemüller, *Phys. Rev. Lett.* **101**, 133004 (2008).
- [18] P. Pedri and L. Santos, *Phys. Rev. Lett.* **95**, 200404 (2005); F. Maucher, N. Henkel, M. Saffman, W. Krolikowski, S. Skupin, and T. Pohl, *ibid.* **106**, 170401 (2011); F. Maucher, S. Skupin, M. Shen, and W. Królikowski, *Phys. Rev. A* **81**, 063617 (2010).
- [19] T. Lahaye, C. Menotti, L. Santos, M. Lewenstein, and T. Pfau, *Rep. Prog. Phys.* **72**, 126401 (2009).
- [20] T. P. Simula and P. B. Blakie, *Phys. Rev. Lett.* **96**, 020404 (2006); Z. Hadzibabic, P. Krüger, M. Cheneau, B. Battelier, and J. Dalibard, *Nature (London)* **441**, 1118 (2006); M. J. Davis, S. A. Morgan, and K. Burnett, *Phys. Rev. A* **66**, 053618 (2002); N. G. Berloff and B. V. Svistunov, *ibid.* **66**, 013603 (2002); S.-W. Su, S.-C. Gou, A. Bradley, O. Fialko, and J. Brand, *Phys. Rev. Lett.* **110**, 215302 (2013); P. M. Chesler, A. M. García-García, and H. Liu, *Phys. Rev. X* **5**, 021015 (2015).
- [21] V. I. Yukalov, A. N. Novikov, and V. S. Bagnato, *J. Low Temp. Phys.* **180**, 53 (2015); E. A. L. Henn, J. A. Seman, G. Roati, K. M. F. Magalhães, and V. S. Bagnato, *Phys. Rev. Lett.* **103**, 045301 (2009); *J. Low Temp. Phys.* **158**, 435 (2009); T. W. Neely, A. S. Bradley, E. C. Samson, S. J. Rooney, E. M. Wright, K. J. H.

- Law, R. Carretero-González, P. G. Kevrekidis, M. J. Davis, and B. P. Anderson, *Phys. Rev. Lett.* **111**, 235301 (2013); T. Simula, M. J. Davis, and K. Helmersson, *ibid.* **113**, 165302 (2014); W. J. Kwon, G. Moon, J. Y. Choi, S. W. Seo, and Y.-i. Shin, *Phys. Rev. A* **90**, 063627 (2014); W. J. Kwon, G. Moon, S. W. Seo, and Y. Shin, *ibid.* **91**, 053615 (2015); G. W. Stagg, A. J. Allen, N. G. Parker, and C. F. Barenghi, *ibid.* **91**, 013612 (2015).
- [22] N. G. Parker, B. Jackson, A. M. Martin, and C. S. Adams, *Vortices in Bose-Einstein Condensates: Theory, Emergent Non-linear Phenomena in Bose-Einstein Condensates* (Springer, Berlin, 2008); N. T. Zinner, *Phys. Res. Int.* **2011**, 734543 (2011); F. Federici, C. Cherubini, S. Succi, and M. P. Tosi, *Phys. Rev. A* **73**, 033604 (2006); F. Kühnel and C. Rampf, *Phys. Rev. D* **90**, 103526 (2014); T. Harko, *ibid.* **89**, 084040 (2014).
- [23] K. T. Kapale and J. P. Dowling, *Phys. Rev. Lett.* **95**, 173601 (2005); S. Thanvanthri, K. T. Kapale, and J. P. Dowling, *Phys. Rev. A* **77**, 053825 (2008).
- [24] S. Thanvanthri, K. T. Kapale, and J. P. Dowling, *J. Mod. Opt.* **59**, 1180 (2012).
- [25] Z. F. Xu, P. Zhang, R. Lü, and L. You, *Phys. Rev. A* **81**, 053619 (2010).
- [26] Y.-Z. Zhang, J. Luo, and Y.-X. Nie, *Mod. Phys. Lett. A* **16**, 789 (2001); C. Jacinto de Matos, *J. Supercond. Nov. Magn.* **24**, 193 (2011).
- [27] E. C. Samson, K. E. Wilson, Z. L. Newman, and B. P. Anderson, *Phys. Rev. A* **93**, 023603 (2016).
- [28] A. A. Svidzinsky and A. L. Fetter, *Phys. Rev. Lett.* **84**, 5919 (2000); A. L. Fetter, *Rev. Mod. Phys.* **81**, 647 (2009); P. Kuopanportti, E. Lundh, J. A. M. Huhtamäki, V. Pietilä, and M. Möttönen, *Phys. Rev. A* **81**, 023603 (2010); P. Kuopanportti and M. Möttönen, *ibid.* **81**, 033627 (2010).
- [29] M. Quiroga-Teixeiro and H. Michinel, *J. Opt. Soc. Am. B* **14**, 2004 (1997); R. L. Pego and H. A. Warchall, *J. Nonlin. Sci.* **12**, 347 (2002); A. S. Reyna, G. Boudebs, B. A. Malomed, and C. B. de Araújo, *Phys. Rev. A* **93**, 013840 (2016).
- [30] H. Sakaguchi, B. Li, and B. A. Malomed, *Phys. Rev. E* **89**, 032920 (2014); L. Salasnich, W. B. Cardoso, and B. A. Malomed, *Phys. Rev. A* **90**, 033629 (2014); H. Sakaguchi, E. Y. Sherman, and B. A. Malomed, *Phys. Rev. E* **94**, 032202 (2016).
- [31] Y.-C. Zhang, Z.-W. Zhou, B. A. Malomed, and H. Pu, *Phys. Rev. Lett.* **115**, 253902 (2015).
- [32] F. Dalfvo and S. Stringari, *Phys. Rev. A* **53**, 2477 (1996); T. J. Alexander and L. Bergé, *Phys. Rev. E* **65**, 026611 (2002); L. D. Carr and C. W. Clark, *Phys. Rev. Lett.* **97**, 010403 (2006); D. Mihalache, D. Mazilu, B. A. Malomed, and F. Lederer, *Phys. Rev. A* **73**, 043615 (2006).
- [33] O. V. Borovkova, Y. V. Kartashov, L. Torner, and B. A. Malomed, *Phys. Rev. E* **84**, 035602(R) (2011); R. Driben, Y. V. Kartashov, B. A. Malomed, T. Meier, and L. Torner, *Phys. Rev. Lett.* **112**, 020404 (2014).
- [34] J. B. Sudharsan, R. Radha, H. Fabrelli, A. Gammal, and B. A. Malomed, *Phys. Rev. A* **92**, 053601 (2015).
- [35] L. Bergé, *Phys. Rep.* **303**, 259 (1998); E. A. Kuznetsov and F. Dias, *ibid.* **507**, 43 (2011).
- [36] C. Josserand, *Chaos* **14**, 875 (2004); J.-k. Kim and A. L. Fetter, *Phys. Rev. A* **72**, 023619 (2005); P. Kuopanportti and M. Möttönen, *J. Low Temp. Phys.* **161**, 561 (2010); D.-S. Wang, S.-W. Song, B. Xiong, and W. M. Liu, *Phys. Rev. A* **84**, 053607 (2011); Y. Zhao, J. An, and C.-D. Gong, *ibid.* **87**, 013605 (2013); P. Kuopanportti, N. V. Orlova, and M. V. Milošević, *ibid.* **91**, 043605 (2015).
- [37] S. Inouye, M. R. Andrews, J. Stenger, H.-J. Miesner, D. M. Stamper-Kurn, and W. Ketterle, *Nature (London)* **392**, 151 (1998); T. Kohler, K. Goral, and P. S. Julienne, *Rev. Mod. Phys.* **78**, 1311 (2006); C. C. Chin, R. Grimm, P. Julienne, and E. Tsieng, *ibid.* **82**, 1225 (2010).
- [38] L. Radzihovsky and D. E. Sheehy, *Rep. Prog. Phys.* **73**, 076501 (2010); X.-W. Guan, M. T. Batchelor, and C. Lee, *Rev. Mod. Phys.* **85**, 1633 (2013).
- [39] B. D. Esry, C. H. Greene, J. P. Burke, and J. L. Bohn, *Phys. Rev. Lett.* **78**, 3594 (1997); M. L. Chiofalo, S. Succi, and M. P. Tosi, *Phys. Rev. E* **62**, 7438 (2000); W. Bao and Q. Du, *SIAM J. Sci. Comput.* **25**, 1674 (2004).
- [40] R. M. Caplan, Q. E. Hoq, R. Carretero-González, and P. G. Kevrekidis, *Opt. Commun.* **282**, 1399 (2009); R. M. Caplan, R. Carretero-González, P. G. Kevrekidis, and B. A. Malomed, *Math. Comput. Simul.* **82**, 1150 (2012).
- [41] R. Y. Chiao, E. Garmire, and C. H. Townes, *Phys. Rev. Lett.* **13**, 479 (1964).
- [42] V. I. Kruglov, Y. A. Logvin, and V. M. Volkov, *J. Mod. Opt.* **39**, 2277 (1992).
- [43] F. Maucher, S. Skupin, and W. Krolikowski, *Nonlinearity* **24**, 1987 (2011).
- [44] D. E. Pelinovsky, Y. S. Kivshar, and V. V. Afanasjev, *Physica D* **116**, 121 (1998); Y. S. Kivshar, D. E. Pelinovsky, T. Cretegny, and M. Peyrard, *Phys. Rev. Lett.* **80**, 5032 (1998).
- [45] E. V. Doktorov, *Phys. Lett. A* **374**, 247 (2009).
- [46] F. Maucher, E. Siminos, W. Krolikowski, and S. Skupin, *New J. Phys.* **15**, 083055 (2013).
- [47] W. J. Firth and D. V. Skryabin, *Phys. Rev. Lett.* **79**, 2450 (1997).
- [48] H. Saito and M. Ueda, *Phys. Rev. Lett.* **89**, 190402 (2002).
- [49] Y. S. Kivshar and G. P. Agrawal, *Optical Solitons: From Fibers to Photonic Crystals* (Academic, San Diego, 2003).
- [50] M. Brtko, A. Gammal, and B. A. Malomed, *Phys. Rev. A* **82**, 053610 (2010).
- [51] R. Zeng and Y. Z. Zhang, *Comput. Phys. Commun.* **180**, 854 (2009).